22nd International Symposium on Plasma Chemistry
July 5-10, 2015; Antwerp, Belgium

How does N_2 influence the CO_2 conversion and energy efficiency in a dielectric barrier discharge and microwave plasma?

R. Snoeckx[1], S. Heijkers[1], T. Kozák[1,2], K. Van Wesenbeeck[3], R. Aerts[1], T. Silva[4], T. Godfroid[5], N. Britun[4], S. Lenaerts[3], R. Snyders[4,5] and A. Bogaerts[1]

[1] *Research group PLASMANT, Department of Chemistry, University of Antwerp, 2610 Antwerpen-Wilrijk, Belgium*
[2] *Department of Physics and NTIS, European Centre of Excellence, University of West Bohemia, Univerzitní 8, 30614 Plzeň, Czech Republic*
[3] *Research group DuEL, Department of Bioscience Engineering, University of Antwerp, 2020 Antwerpen, Belgium*
[4] *Chimie des Interactions Plasma-Surface (ChIPS), CIRMAP, Université de Mons, 7000 Mons, Belgium*
[5] *Materia Nova Research Center, Parc Initialis, 7000 Mons, Belgium*

Abstract: A combined computational and experimental study is presented to compare a dielectric barrier discharge and microwave plasma operating in a CO_2/N_2 mixture. More specifically, we study the CO_2 and N_2 conversion, as well as the energy efficiency, for different N_2 fractions in the gas mixture. Both the conversion and energy efficiency are much better in the microwave plasma, due to the important role of the vibrational levels, but a significant fraction of N_2 is also converted into unwanted NO_x compounds.

Keywords: CO_2, N_2, NO_x, dielectric barrier discharge, microwave plasma

1. Introduction

The conversion of the main greenhouse gases CO_2 and CH_4 into value added chemicals and liquid fuels is one of the main challenges for the 21st century. As a result, interest for gas conversion technology has grown quickly in the past decade and a technology considered to have great potential in this area is plasma technology [1]. Currently, CH_4 reforming and CO_2 splitting processes are considered a hot topic both from an economic and ecological point of view [2]. So it is not surprising that a lot of research effort has already been put into non-thermal atmospheric plasmas for this purpose. However, most studies focus on "clean" pure gases, while in reality most gases and industrial gas flows contain impurities, for which it is economically unfeasible to remove them. CO_2 gas flows from industrial and Carbon Capture Storage & Utilisation/Reuse often contain impurities, of which in most cases nitrogen is the most important component [3].

Therefore, it is of great importance to study the effect of N_2 on the CO_2 conversion. The following specific questions need to be answered: how does N_2 affect the conversion and energy efficiency, and which products (e.g., useful products or harmful NO_x compounds) would be formed. These questions can be answered by experiments. Different types of plasmas have been proposed for this purpose, but a dielectric barrier discharge (DBD) and microwave (MW) plasma are most often used [4]. Therefore, we investigated the effect of N_2 as impurity (1 to 10 %) for CO_2 splitting for both a DBD and a MW setup, to compare both setups by evaluating the conversion of the reactants, the selectivity of the main products and the overall energy efficiency. Furthermore, we investigated the effect of N_2 as admixture or as dilutant (1 to 99%), to see whether nitrogenated compounds are formed, which could be of interest for the chemical industry.

2. Description of the Model

2.1. 0D Chemical Kinetics Model

We used a zero-dimensional (0D) chemical kinetics model, called ZDPlaskin [5], which calculates the time-evolution of the species densities by balance equations, based on the various production and loss terms by chemical reactions. The rate coefficients of these reactions are adopted from literature for the heavy particle reactions, while they are calculated with a Boltzmann solver, BOLSIG+ [6], for the electron impact reactions. Scaling theories, i.e., the Forced Harmonic Oscillator (FHO) theory [7] and the Schwartz, Slawsky and Herzfeld (SSH)-theory [8], are used to calculate the rate coefficients of vibration induced reactions with highly vibrationally excited species, from the rate coefficients of these reactions with the species residing in the lowest vibrational levels.

2.2. Plasma Chemistry Included in the Model

Our model is based on the reaction kinetics model developed earlier for the dissociation of pure CO_2 in a MW plasma and a dielectric barrier discharge [9, 10], including state-to-state reactions of vibrational levels of CO_2 and CO, and it is extended to a CO_2/N_2 mixture. The species included in our model are various neutral molecules in the ground state, as well as electronic and vibrationally excited levels of CO_2, CO, N_2 and O_2, various radicals, positive and negative ions, and electrons. Besides the input gases (CO_2 and N_2), also various formed products are included, such as CO, O_2, O_3, several NO_x compounds, as well as some other CO_2-

derived compounds, N-C and N-C-O compounds. Because the asymmetric mode levels are most important for the splitting of CO_2 [7, 8], all these levels up to the dissociation limit are included in the model (i.e., 21 levels), whereas only a few symmetric mode levels are incorporated, following the example of the model developed by Kozák *et al.* [9]. In the case of N_2, 14 levels are used. More details about the MW-model can be found in the work of Heijkers *et al.* [4] and about the DBD-model in the work of Snoeckx *et al.* [13].

3. Experimental

3.1. DBD set-up

The experiments are carried out in a cylindrical DBD reactor, consisting of an inner electrode and a coaxial alumina tube, which is covered by a stainless steel mesh electrode. The outer electrode is connected to a high voltage output and the inner electrode is grounded via an external capacitor (48 nF). The length of the discharge region is 90 mm and the discharge gap is fixed at 1.8 mm, resulting in a discharge volume of 7.4 cm^3. CO_2 and N_2 are used as feed gases with a constant total flow rate of 611 ml min^{-1} and N_2 content of 0-10 % in steps of 1 %, 10-90 % in steps of 10 % and 90-100 % again in steps of 1 %, controlled with mass flow controllers (Bronkhorst). The DBD reactor is powered by an AC high-voltage power supply (AFS), providing a peak-to-peak voltage of 11-12 kV at a frequency of 23.5 kHz. The applied voltage (U_a) is measured by a high voltage probe, while the total current (I_t) is recorded by a Rogowski-type current monitor (Pearson 4100). The voltage on the external capacitor (U_c) is measured to obtain the charge generated in the discharge and all the electrical signals are sampled by a four-channel digital oscilloscope (Picotech PicoScope). A control system is used for the measurement of the discharge power (110-130 W) by the area calculation of the Q-U Lissajous figures.

3.2. MW set-up

The experiments are done in a microwave discharge generated with a 915 MHz microwave generator in a double-walled quartz tube with 14 mm inner diameter and about 20 cm length at an initial gas temperature of 300 K, a pressure of 2660 Pa, gas fractions ranging from 0 till 90 %, a gas flow rate of 5 slm and a power density of 30 W/cm^3.

3.3. Product Analysis

The evolution of the concentrations of CO_2, CO, O_2 and N_2 was analyzed by gas chromatography.

Furthermore an FTIR-spectrometer was used to follow the formation (and concentration) of O_3 and NO_x compounds, such as NO, NO_2, N_2O and to a lower extent also N_2O_3 and N_2O_5.

3.4. Energy Input Comparison

To compare both set-ups, we should make sure that we use the appropriate unit of measurement. Several different units of energy are described in literature, such as: power density (W/cm^3), specific energy input (J/cm^3), specific energy input (eV/molecule). We chose to compare both set-ups based on the SEI in eV/molecule, since this is the most "fundamental" comparison. Indeed, this tells us exactly how much energy is going to each molecule (on average). If we take a look at Table 1, it also becomes clear why this is the logical approach. The other units would give us a distorted view, since both setups have completely different operating parameters, especially regarding pressure and temperature. For example, if we look at the SEI in J/cm^3, the MW is clearly operating in a much lower range, however, due to the low pressure (2660 Pa), there are much less molecules per volume and thus the SEI in eV/molecule is much higher. Another reason why we will compare the DBD experiments with the MW experiments based on the SEI expressed in eV/molecule, is that when the temperature increases in the set-ups, the residence times change, but the SEI expressed in eV/molecule does not change, since this effect is counteracted by the decrease in number of molecules per volume due to the temperature change at constant pressure (pV = nRT).

Table 1. Energy input comparison for DBD and MW.

	DBD	**MW**
Power density (W/cm^3)	14.9 - 17.6	30
SEI (J/cm^3)	10.8 – 12.8	0.27
SEI (eV/molecule)	2.51 - 2.97	2.66

4. Results and Discussion

As mentioned above, both the model and experiments are applied to a DBD reactor and a MW plasma, in a wide range of CO_2/N_2 gas mixing ratios. We will first compare the CO_2 conversion and the energy efficiency in both reactors. Subsequently, we will analyze the destruction and formation processes of CO_2, to explain the differences observed for both reactors. Finally, we will present the most important products formed in both reactors.

4.1. Conversion and Energy Efficiency

Fig. 1 illustrates the calculated and experimental absolute CO_2 conversion as a function of the N_2 content for both the DBD and MW plasma. The absolute CO_2 conversion increases with rising N_2 fraction, both in the calculations and the experimental data. The shape of the curve shows a more or less exponential increase for both the DBD and MW plasma. For both the DBD and MW model, the exact trends are somewhat different from the experiments, indicating that the underlying chemistry might not yet be 100% captured in the model, but the absolute values are in reasonable agreement. These rising trends indicate that N_2 has a beneficial effect on the CO_2 splitting, as we will illustrate in section 4.2 below.

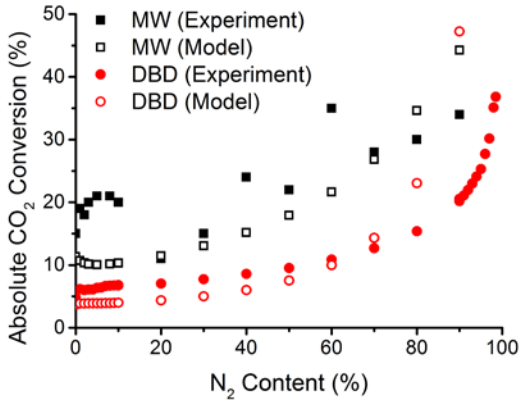

Fig. 1. Calculated and experimental absolute CO_2 conversion as a function of the N_2 content for both the DBD and MW plasma.

Fig. 2, on the other hand, illustrates the calculated and experimental effective CO_2 conversion as a function of the N_2 content for both the DBD and MW plasma. The effective or overall CO_2 conversion remains relatively constant around 4 % for the DBD and 9 % for the MW (and slightly higher for both the experimental data). This is logical, because the absolute conversion increases, but the fraction of CO_2 in the gas mixture decreases, so the effective conversion remains more or less constant. In other words, the increase in absolute conversion by adding N_2 is high enough to counteract the lower CO_2 concentration.

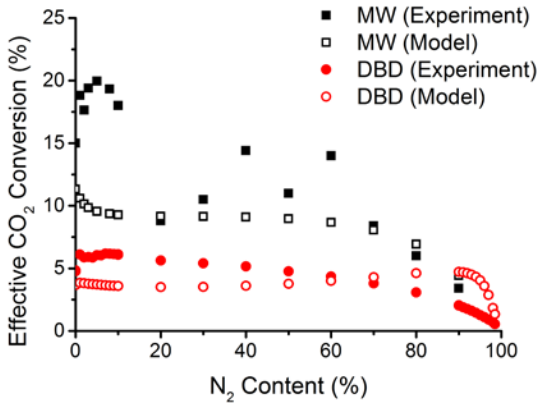

Fig. 2. Calculated and experimental effective CO_2 conversion as a function of the N_2 content for both the DBD and MW plasma.

From Figs. 1 and 2 it also becomes clear that although we are putting in almost exactly the same amount of energy per molecule, the CO_2 conversion in the MW is a factor 2-3 higher than for the DBD. This also results in a 2-3 times higher energy efficiency for the MW plasma (see Fig. 3). The reason for this will be further explained in section 4.2 below.

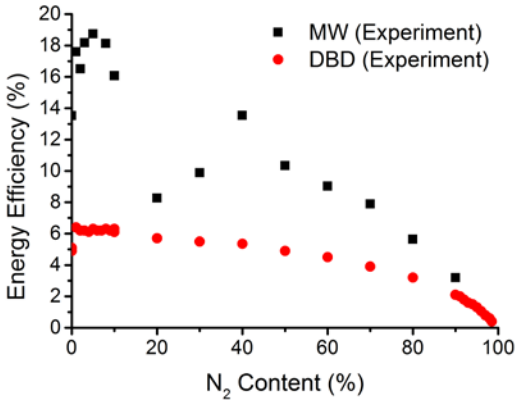

Fig. 3. Experimental energy efficiency as a function of the N_2 content for both the DBD and MW plasma.

4.2. Destruction Processes of CO_2

The most important destruction processes for CO_2 are listed in Table 2 for the DBD reactor and in Table 3 for the MW plasma.

Table 2. Overview of the most important destruction processes of CO_2 in the DBD reactor.

No.	Destruction process
1	$e^- + CO_2 \rightarrow CO + O + e^-$
2	$e^- + CO_2\,(v) \rightarrow CO + O + e^-$
3	$CO_2 + N_2(A^3\Sigma_u^+) \rightarrow CO + O + N_2$
4	Reactions with positive ions
5	$CO_2\,(v) + N_2(A^3\Sigma_u^+) \rightarrow CO + O + N_2$
6	$e^- + CO_2 \rightarrow CO_2^+ + e^- + e^-$
7	Reactions with negative ions

Table 3. Overview of the most important destruction processes of CO_2 in the MW plasma.

No.	Destruction process
1	$CO_2\,(v) + M \rightarrow CO + O + M$
2	$e^- + CO_2 \rightarrow CO + O + e^-$
3	$e^- + CO_2\,(v) \rightarrow CO + O + e^-$
4	$CO_2\,(v) + O \rightarrow CO + O_2$

Hence, from Tables 2 and 3 it becomes clear that in the MW plasma CO_2 is mainly destroyed by processes of vibrationally excited CO_2 levels, which are mostly negligible in the DBD reactor. Indeed, the vibrational levels are much more populated in a MW plasma than in a DBD reactor, as was demonstrated by Kozák *et al.* for a pure CO_2 plasma [10]. This effect seems to be even more pronounced when N_2 is present, because N_2 helps to populate the CO_2 vibrational levels, by VV relaxation

processes, as discussed in detail in [4]. As the CO_2 dissociation processes with vibrationally excited levels are much more energy efficient than electron impact dissociation, certainly from the ground state, this explains the higher CO_2 conversion and energy efficiency in a MW plasma than in a DBD reactor (cf. Figs. 1 and 2).

4.3. Analysis of the Formed Products

CO_2 splitting typically yields the formation of CO and O_2 molecules; the latter being formed by the recombination of O atoms. Besides, also O_3 can be created [14]. However, in the presence of N_2, also NO_x compounds might be produced. Therefore, it is of crucial importance to analyze the product formation in the CO_2/N_2 plasma, and to compare the results for the DBD and MW plasma.

From both the modeling and experimental results it becomes clear that several NO_x compounds are produced, especially NO, NO_2 and N_2O, while the other NO_x compounds are more or less negligible. Although their concentrations remain in the ppm range, this is not unimportant, since they give rise to several environmental problems. N_2O is an even more potent greenhouse gas than CO_2 (with a global warming potential of 300 CO_{2eq}), while NO and NO_2 are responsible for acid rain and the formation of ozone and a wide variety of toxic products.

Due to the higher conversion in the MW plasma, the formation of NO_x compounds also appears to be higher than for the DBD reactor. These results indicate that in a MW plasma, even more than in a DBD reactor, it appears to be crucial to separate the CO_2 gas from N_2 impurities (or gas fractions) before plasma treatment, to avoid the formation of NO_x compounds.

5. Conclusions

The absolute CO_2 conversion in the DBD and MW plasma show an increasing trend, with the latter being 2-3 times as high as the former. However, because the initial fraction of CO_2 in the gas mixture decreases with rising N_2 fraction, the effective CO_2 conversion remains more or less constant in both cases, i.e., around 4% in the DBD reactor and around 9% in the MW plasma.

The rise in the absolute CO_2 conversion upon increasing N_2 fraction in both plasma reactors indicates that N_2 has a beneficial effect on the CO_2 splitting, but the mechanism differs. In the DBD reactor, this is because of the reaction with electronically excited $N_2(A^3\Sigma_u^+)$. In the MW plasma, CO_2 is mainly converted by processes of vibrationally excited CO_2 levels. These levels are much more populated in a MW plasma than in a DBD reactor, and this appears especially true for a CO_2/N_2 gas mixture, because N_2 helps populating the CO_2 vibrational levels by VV relaxation processes. As the CO_2 dissociation from vibrationally excited levels is much more efficient than dissociation from the ground state, this also explains the higher CO_2 conversion and consequently also the higher energy efficiency for the MW plasma than for the DBD reactor.

Finally, reactive NO_x are formed in both the DBD and MW plasma. Although they remain in the ppm level, they give rise to several environmental problems. This indicates that it might be beneficial to use purified CO_2 to circumvent expensive end-of-pipe denox installations.

6. Acknowledgements

The authors acknowledge financial support from the IAP/7 (Inter-university Attraction Pole) program 'PSI-Physical Chemistry of Plasma-Surface Interactions' by the Belgian Federal Office for Science Policy (BELSPO) and from the Fund for Scientific Research Flanders (FWO). The calculations were performed using the Turing HPC infrastructure at the CalcUA core facility of the Universiteit Antwerpen, a division of the Flemish Supercomputer Center VSC, funded by the Hercules Foundation, the Flemish Government (department EWI) and the Universiteit Antwerpen. N.B. is a post-doctoral researcher of FNRS, Belgium.

7. References

[1] S. Samukawa, *et al. J. Phys. D: Appl. Phys.*, **45**, 253001 (2012)

[2] G. Centi, E.A. Quadrelli and S. Perathoner *Energy Environ. Sci.*, **6**, 1711 (2013)

[3] M. Aresta, A. Dibenedetto and A. Angelini. *Chem. Rev.*, **114**, 1709-1742 (2014)

[4] S. Heijkers, R. Snoeckx, T. Kozák, T. Silva, T. Godfroid, N. Britun, R. Snyders and A. Bogaerts. *J. Phys. Chem. C*, submitted (2015)

[5] S. Pancheshnyi, B. Eismann, G.J.M. Hagelaar and L.C. Pitchford. *DPlasKin: a new tool for plasmachemical simulations.* (2008)

[6] G.J.M. Hagelaar and L.C. Pitchford. *Plasma Sources Sci. Technol.*, **14**, 722-733 (2005)

[7] I.V. Adamovich, S.O. MacHeret, J.W. Rich and C. E. Treanor. *J. Thermophys. Heat Transf.*, **12**, 57-65 (1998)

[8] R.N. Schwartz, Z.I. Slawsky and K.F. Herzfeld. *J. Chem. Phys.*, **20**, 1591 (1952)

[9] T. Kozák and A. Bogaerts. *Plasma Sources Sci. Technol.*, **23**, 045004 (2014)

[10] T. Kozak and A. Bogaerts. *Plasma Sources Sci. Technol.*, **24**, 015024 (2015)

[11] A. Fridman. *Plasma chemistry*. (New York: Cambridge University Press) pp. 1022 (2008)

[12] V.D. Rusanov, A.A. Fridman and G.V. Sholin. *Uspekhi Fiz. Nauk*, **134**, 185 (1981)

[13] R. Snoeckx, S. Heijkers, T. Kozák, R. Aerts, T. Silva, T. Godfroid, N. Britun, R. Snyders and A. Bogaerts. "Influence of N2 concentration in a CO2/N2 dielectric barrier discharge and microwave plasma used for CO2 splitting". Paper in preparation (2015)

[14] R. Aerts, T. Martens and A. Bogaerts. *J. Phys. Chem. C*, **116**, 23257-23273 (2012)